https://doi.org/10.2352/CIC.2024.32.1.3

CIE Colour Matching Functions and Cone Fundamentals: Problems and Modifications

Cheng Gao [1], Kaida Xiao [2]*, Mike Pointer [2] and Changjun Li [1,2]
1 University of Science and Technology Liaoning, Anshan, China
2 University of Leeds, Leeds, United Kingdom
**** Correspondence email: k.xiao1@leeds.ac.uk***

Abstract

CIE colorimetry based on colour matching functions has been successfully applied in various industrial applications. In the past it was generally accepted that the chromaticity diagram based on either 1931 or 1964 colour matching functions (CMFs), contains all the chromaticity coordinates of stimuli, which means the domain (Ω) enclosed by the spectrum locus and the purple line is convex. Also based on the chromaticity diagram, the Helmholtz coordinates (dominant wavelength and excitation purity) can be defined. In this paper, these properties of chromaticity coordinates based on CIE 1931, CIE 1964, CIE 2006 2- and 10-degree cone fundamentals (CFs) and cone fundamentals-based CMFs are evaluated. It is found that the domain Ω does not contain the chromaticity coordinates of all stimuli, and spectral chromaticity coordinates do not distribute in the wavelength order along the spectrum locus, which results in no way to determine the Helmholtz coordinates for certain stimuli. Finally modified CIE 1931 CMFs, CIE 1964 CMFs, and CFs and CMFs based on CFs, are derived.

Introduction

The CIE colorimetric system [1] was established in 1931. The most important space in the system is the space of tristimulus values (TSV) defined in terms of colour matching functions (CMFs) $\bar{x}(\lambda)$, $\bar{y}(\lambda)$ and $\bar{z}(\lambda)$ by:

$$\begin{cases} X = k\int_a^b E(\lambda)R(\lambda)\bar{x}(\lambda)d\lambda \\ Y = k\int_a^b E(\lambda)R(\lambda)\bar{y}(\lambda)d\lambda \\ Z = k\int_a^b E(\lambda)R(\lambda)\bar{z}(\lambda)d\lambda \end{cases}, \text{ with } k = 100\int_a^b E(\lambda)\bar{y}(\lambda)d\lambda \quad (1)$$

Here, $a = 360$ nm and $b = 830$ nm [1,2], $R(\lambda)$ is the reflectance of the stimulus, and $E(\lambda)$ is the relative spectral power distribution of the illuminant. The earliest set of CMFs is the CIE 1931 CMFs which were derived based on two experimental investigations, conducted by W. D. Wright [3] and J. Guild [4] respectively. For easy recognition of the hue and saturation or chroma of the given stimulus, chromaticity coordinates [1] are defined as:

$$\begin{cases} x = \dfrac{X}{X+Y+Z} \\ y = \dfrac{X}{X+Y+Z} \\ z = \dfrac{X}{X+Y+Z} \end{cases} \quad (2)$$

Since $x + y + z = 1$, normally only the x and y chromaticity coordinates are quoted. A plot of y against x is called a **chromaticity diagram**. Note that, CMFs $\bar{x}(\lambda)$, $\bar{y}(\lambda)$ and $\bar{z}(\lambda)$ are TSVs of monochromatic stimuli, hence chromaticity coordinate $x(\lambda)$ and $y(\lambda)$ can be similarly defined, and they are **called spectral chromaticity coordinates** (SCCs). The curve obtained by connecting the spectral chromaticity points in wavelength order is known as the **spectrum locus** [5-8]. Figure 1 shows the CIE 1931 chromaticity diagram, the curve boundary (dotted curve) is the CIE 1931 spectrum locus. The line linking the two ends of the spectrum locus is the **purple line** [5,6]. Note that here "two ends of the spectrum locus" means SCCs at 360 nm and 830 nm respectively.

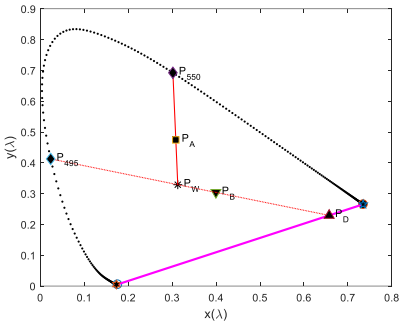

***Figure 1**. The CIE 1931 $(x(\lambda),\ y(\lambda))$ chromaticity diagram. Open circle, solid circle, hexagon and pentagram symbols are SCCs at 360 nm, 830 nm, 404 nm and 829 nm respectively. The line linking the SCC at 360 nm and the SCC at 830 nm is the purple line (magenta). P_W (*) is the chromaticity coordinate of the CIE D65 illuminant , P_A (●) P_B (▼) respectively are the chromaticity coordinates for given samples A and B. Sample A has dominant wavelength $\lambda_d = 550$ nm and B has a complementary wavelength $\lambda_c = 495$ nm. The symbol (▲) indicates the intersection point with chromaticity coordinate denoted by P_D of the purple line and the line going through the points P_W and P_B.*

Note that in the latest edition of the International Lighting Vocabulary [9], one can find that " the purple boundary is a line in a chromaticity diagram, or the plane surface in a tristimulus space, that represents additive mixtures of monochromatic stimuli of wavelengths approximately 380 nm and 780 nm", which we believe is linked to the visible range between 380nm and 780nm.

Firstly, let Ω be the domain or area enclosed by the spectrum locus and purple line. Thus, it is to be expected that Ω should contain chromaticity points of all stimuli, which means Ω should contain all CIE colours.

Next, we note that, because all the integrands involved have no analytical expression, CIE [1] recommends the integrations in Eq. (1) can be replaced by summations with wavelength steps at 1 nm intervals. Thus, if we let

$$\varphi(\lambda) = kE(\lambda)R(\lambda) \quad (3)$$

and

$$s(\lambda) = \bar{x}(\lambda) + \bar{y}(\lambda) + \bar{z}(\lambda) \quad (4)$$

then for any stimulus, its chromaticity coordinates x and y can be expressed as

$$\begin{cases} x = \sum_{\lambda=a}^{b} \alpha(\lambda) x(\lambda) \\ y = \sum_{\lambda=a}^{b} \alpha(\lambda) y(\lambda) \end{cases} \quad (5)$$

In the above equation (5), $x(\lambda)$ and $y(\lambda)$ are SCCs at wavelength λ and $\alpha(\lambda)$ is given by

$$\alpha(\lambda) = \frac{\varphi(\lambda)s(\lambda)}{\sum_{\lambda=a}^{b} \varphi(\lambda)s(\lambda)} \quad (6)$$

Note that summations in Eqs. (5) and (6) are for wavelength λ from a to b with step interval being 1 nm. Thus, we have

$$\sum_{\lambda=a}^{b} \alpha(\lambda) = 1, \text{ and } \alpha(\lambda) \geq 0 \quad (7)$$

Hence, from Eqs. (5)-(7) we can say for any stimulus, its chromaticity coordinates $(x, y)^T$ are the convex combination [10] of the SCCs $(x(\lambda), y(\lambda))^T$. Here, the superscript T denotes the transpose of a vector or matrix.

Since we expect $(x, y)^T$ for all CIE colours to be inside the domain Ω, the CMFs should have the following property:

Property I: Any convex combination of the SCC $(x(\lambda), y(\lambda))^T$ derived from the CMFs should locate inside or on the boundary of the domain Ω.

Note that if the CMFs satisfy Property I, then the domain Ω is convex (the line linking any two points on the spectrum locus is inside the domain Ω). This property is widely admitted in the colour and vision community such as in the book by Hunt and Pointer [6, page 43] and the book edited by McDonald [7, page 107], but, to our knowledge, an evaluation of this property, for the given set of CMFs has not been reported in the literature.

Another property related to the chromaticity diagram relates to the hue and saturation of a given stimulus under a viewing condition combination. Let $P_A = (x, y)^T$ and $P_W = (x_W, y_W)^T$ be chromaticity points for a stimulus A and the illuminant respectively. And let the line linking P_W and P_A intersect the spectrum locus at $P_\lambda = (x(\lambda), y(\lambda))^T$ as shown in Figure 1, where P_W is the chromaticity coordinates of CIE illuminant D65, SCCs at 360 nm and 830 nm are labelled with an open circle and a solid circle respectively. The chromaticity point P_A is a convex combination of the chromaticity points P_W and P_λ, which is considered as the monochromatic stimulus (P_λ) mixed additively with the specified achromatic stimulus (P_W). The corresponding wavelength λ of the monochromatic stimulus is known as the **dominant wavelength** of the given stimulus and is denoted as λ_d. Let $d(P_W, P_A)$ denote the distance between P_W and P_A, then the ratio $d(P_W, P)/d(P_W, P_\lambda)$ is the **excitation purity** p_e. As an approximation [5,8], dominant wavelength λ_d expresses the hue and excitation purity p_e the saturation of the given stimulus. λ_d and p_e are also known as Helmholtz coordinates [5].

The stimulus B labelled with chromaticity coordinates denoted by P_B in Figure 1 has an associated complementary wavelength $\lambda_c = 495$ nm. And the ratio $d(P_{495}, P_B)/d(P_{495}, P_D)$ is the excitation purity for stimulus B.

Note that, for calculating the dominant (or complementary) wavelengths and the excitation purity we tacitly assume the given CMFs have the following property II:

Property II: The line starting at the chromaticity point P_W intersects the spectrum locus at a single wavelength.

That the CMFs, or the chromaticity diagram derived from the CMFs, obeys Property II is important, otherwise a given stimulus may have more than one dominant wavelength, which would not be acceptable. Thus, Property II means that the SCCs must distribute on the spectrum locus strictly in wavelength order from the open circle position to the solid circle position shown in Figure 1.

Next, we want to evaluate the traditional CIE 1931 and 1964 CMFs, the new CIE 2006 cone fundamental (CF) based 2- and 10-degree CMFs, and the CIE 2- and 10- degree cone fundamentals [11,12] to see if they satisfy the above two properties.

Problems with all CIE Colour Matching Functions and Cone Fundamentals

It was found that not all CIE CMFs and CFs do not satisfy the above properties. For example, Figure 2 shows the enlarged shorter (a) and longer (b) wavelength ranges of the chromaticity diagram shown in Figure 1. First, from Figure 2(a), it can be understood that the chromaticity diagram shown in Figure 1 is not convex. Thus CIE 1931 CMFs, or the chromaticity diagram derived from them does not satisfy Property I. Second, from Figure 2(b), it can be seen the SCCs do not distribute in wavelength order. Note that the purple line (solid magenta) linking the SCC with $\lambda = 830$ nm which does not locate at the end of spectrum locus, which means that the domain Ω does not include all CIE colours. Note also that the SCC with $\lambda = 827$ nm locates above the SCC with $\lambda = 830$ nm along the spectrum locus, and the SCC with $\lambda = 829$ nm locates at the end of the spectrum locus. Also, the SCC with $\lambda = 761$ nm and SCC with $\lambda = 830$ nm nearly overlap. The SCCs in the part of spectrum locus between the SCC with $\lambda = 830$ nm and the SCC with $\lambda = 829$ nm do not distribute in wavelength increasing order, which shows the chromaticity diagram shown in Figure 1 does not satisfy Property II.

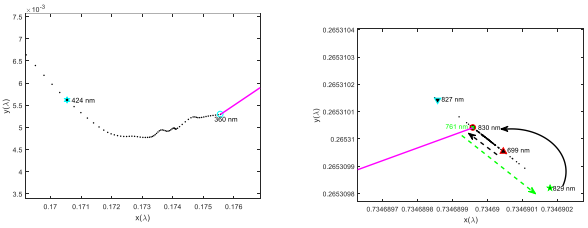

(a) (b)

Figure 2. *Enlargements of the shorter (a) and longer (b) wavelength ranges of the chromaticity diagram shown in Figure 1.*

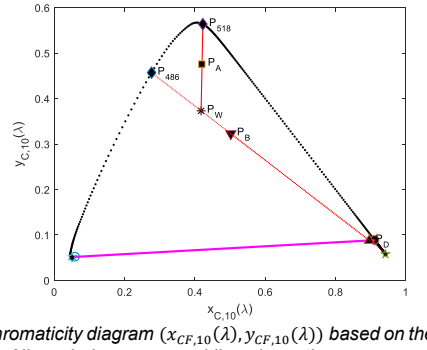

Figure 3. *Chromaticity diagram $(x_{CF,10}(\lambda), y_{CF,10}(\lambda))$ based on the CIE 2006 10-degree CFs. All symbols, curves and lines have the same meanings as those in Figure 1.*

Figures 1 and 2 demonstrate the problems for the chromaticity diagram derived from CIE 1931 CMFs. In addition, it was found all CIE CMFs, cone fundamentals (CFs), and CMFs based on CFs have similar problems. Figure 3 shows the xy chromaticity diagram derived from CIE 2006 10-degree CFs where the chromaticity scales

are represented by $x_{CF,10}(\lambda)$ and $y_{CF,10}(\lambda)$. Here, subscripts CF and 10 denote cone fundamental and 10-degree respectively. All symbols, curves and lines have the same meanings as those in Figure 1. However, in this case, the hexagonal symbol is for SCC at 410 nm, the open circle is SCC at 390 nm and the solid pentagram symbol is for SCC at 703 nm. The solid circle is the SCC at 830 nm. Thus, the purple (magenta) line links the solid and open circles. Again, the SCC at 830 nm does not locate at the end of spectrum locus. Hence the domain Ω does not contain all CIE colours.

Figure 4 shows the enlarged parts around the shorter (a) and longer (b) wavelength ranges of the chromaticity diagram shown in Figure 3. Figure 4(a) shows clearly the domain Ω is not convex. Notice again in Figure 4(b), the solid pentagram is the SCC at 703 nm, the solid circle is the SCC at 830 nm, and the solid circle is located between the SCC at 646 nm and the SCC at 647 nm. Thus, SCCs between 647 nm and 703 nm, and SCCs from 703 nm to 830 nm overlap. Furthermore, the purple line links the solid circle rather than solid pentagram. All these facts cause problems with sample B. It can have a complementary wavelength $\lambda_c = 486$ nm since the dotted red line intersects with purple line at the upper solid triangle with a chromaticity denoted by P_D . But it can also have two dominant wavelengths since the dotted red line intersects with the spectrum locus in the SCCs with shorter and longer wavelength overlaping range. Hence, the dominant wavelength is not unique.
Figures 1-4 show the chromaticity diagrams derived from $\bar{x}(\lambda)$, $\bar{y}(\lambda)$ and $\bar{z}(\lambda)$ and from the $\bar{l}_{10}(\lambda)$, $\bar{m}_{10}(\lambda)$ and $\bar{s}_{10}(\lambda)$, do not satisfy the two properties discussed above. In fact, the problems exist for an xy chromaticity diagram derived from other CMFs and CFs. Furthermore, similar problems exist for other chromaticity diagrams such as uv, $u'v'$, and MacLeod–Boynton Chromaticity Diagram [11,12].

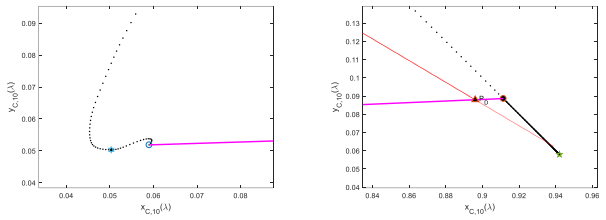

(a) (b)

Figure 4*. Enlarged parts around the shorter (a) and longer (b) wavelength ranges of the chromaticity diagram shown in Figure 3.*

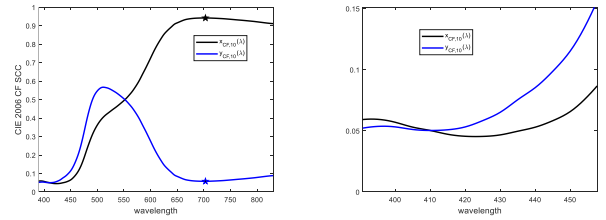

(a) (b)

Figure 5. *(a) Spectral Chromaticity Coordinates $x_{CF,10}(\lambda)$ (black) and $y_{CF,10}(\lambda)$ (blue) based on CIE 2006 10-degree CF versus wavelength (horizontal axis), solid pentagram symbol corresponds to wavelength at 703nm; (b) The enlarged part of Figure 5(a) for shorter wavelength range.*

Modifications to all CIE CMFs and CFs

Though CIE CMFs have been used for many years, the above discussion show they are not perfect in theory. In addition, for CIE 2006 2- and 10-degree CFs， and for CMFs based on CFs, which are defined between 390 nm and 830 nm, further extensions down to 360nm are necessary. Thus, the question to asked is can they be modified so that they satisfy the two properties? We will use the $\bar{l}_{10}(\lambda)$, $\bar{m}_{10}(\lambda)$ and $\bar{s}_{10}(\lambda)$ CFs as an example to illustrate the cause of the problems. Figure 5(a) shows the SCC $x_{CF,10}(\lambda)$ (black) and $y_{CF,10}(\lambda)$ (blue) based on the CIE 2006 10-degree CF, plotted versus wavelength (horizontal axis), and Figure 5(b) shows the enlarged part of Figure 5(a) for the shorter wavelength range. The pentagram symbols correspond to a wavelength at 703 nm. It can be seen that $y_{CF,10}(\lambda)$ peaks at approximately 510 nm, and it has been found that the assumed maximum of $y_{CF,10}(\lambda)$ is at 511 nm. Thus, we can assume that the top of the spectrum locus (see Figure 3) occurs at 511 nm. Figure 3 also shows there is no problem for the spectrum locus in the middle wavelength range, for example between 425 nm and 703 nm and, in this middle wavelength range, it can be seen from Figure 5(a) that, 1) $y_{CF,10}(\lambda)$ decreases monotonically when the wavelength either increases or decreases from 511 nm until a shorter wavelength of 425 nm and a longer wavelength of 703 nm; 2) $x_{CF,10}(\lambda)$ increases monotonically from 425 nm to 703 nm.

Figure 4(a) shows that the problem for the spectrum locus occurs in the shorter wavelength range. In this wavelength range, the spectrum locus assumes its minimum at a wavelength of 410 nm labelled with the solid hexagon symbol, where $y_{CF,10}(\lambda)$ assumes its minimum value (see Figure 5(b)). And between 410 nm and 390 nm $y_{CF,10}(\lambda)$ has a second peak, Figure 5(b). It is this second peak in $y_{CF,10}(\lambda)$ that causes the problem between 410 nm and 390 nm. Furthermore, from Figure 5(b), it can be seen that $x_{CF,10}(\lambda)$ assumes its minimum at wavelength 423 nm, and between 423 nm and 390 nm $x_{CF,10}(\lambda)$ also has a second peak, which causes the non-convex problem shown in Figure 4(a).

Figures 4(b) and 5(a) show that the SCCs with shorter and longer wavelengths cause the overlap problem for the spectrum locus in the wavelength range from 646 nm to 830 nm. Figure 5(a) clearly shows $x_{CF,10}(\lambda)$ increases monotonically with the increasing wavelength from, for example, 430 nm to 703 nm. It can be seen that $x_{CF,10}(\lambda)$ peaks at a wavelength of 703 nm, labelled with a pentagram symbol, and $y_{CF,10}(\lambda)$ assumes its local minimum at a wavelength 703 nm labelled with a pentagram symbol, which cause the SCCs with shorter and longer wavelengths to overlap in this wavelength range, i.e., the SCCs distributes in wavelength in increasing order from 647 nm downward to 703 nm, as shown in Figures 5(a) and 4(b), then from 703 nm upwards to 830 nm.

Based on the above observations, we can establish some principles for modifying $\bar{l}_{10}(\lambda)$, $\bar{m}_{10}(\lambda)$ and $\bar{s}_{10}(\lambda)$.

1): Change $\bar{l}_{10}(\lambda)$, $\bar{m}_{10}(\lambda)$ and $\bar{s}_{10}(\lambda)$ as little as possible;
2): Let $x_{CF,10}(\lambda)$ have one trough at a wavelength of 423 nm and, when λ is away from 423 nm, let $x_{CF,10}(\lambda)$ increase monotonically;
3): Let $y_{CF,10}(\lambda)$ have one peak at 511 nm and one trough at 410 nm, $y_{CF,10}(\lambda)$ then should vary monotonically when λ is between 360 nm and 410 nm, or between 410 nm and 511 nm, or between 511 nm and 830 nm.

For other CIE CMFs and CF, similar principles can be established based on similar observations.

Based on the above principles we have established a nonlinear constrained optimization problem and by the use of numerical solutions we have successfully described modifications to the CIE 1931 and 1964 CMFs, and modifications and extensions to the CIE

2006 2- and 10-degree CFs and CMFs based on CFs. All the modified versions use a capital M in front of the original notions. For example, $M\bar{l}_{10}(\lambda)$ is the modification to $\bar{l}_{10}(\lambda)$, and $M\bar{x}(\lambda)$ is the modification to $\bar{x}(\lambda)$ etc.

Comparisons between original and modified CIE CMFs and CFs

Figure 6(a) shows the original $\bar{x}(\lambda)$, $\bar{y}(\lambda)$ and $\bar{z}(\lambda)$ with solid curves and modified $M\bar{x}(\lambda)$, $M\bar{y}(\lambda)$ and $M\bar{z}(\lambda)$ with dotted curves. Figure 7 shows the enlarged shorter (a) and longer (b) wavelength ranges of the chromaticity diagram derived from the modified $M\bar{x}(\lambda)$, $M\bar{y}(\lambda)$ and $M\bar{z}(\lambda)$. Comparing with Figure 2, it can be seen that the convex property in the shorter wavelength range is satisfied (Figure 7(a)) and SCCs with wavelengths in the wavelength range from 699 nm to 830 nm (see Figure 7(b)) have no overlapping problem.

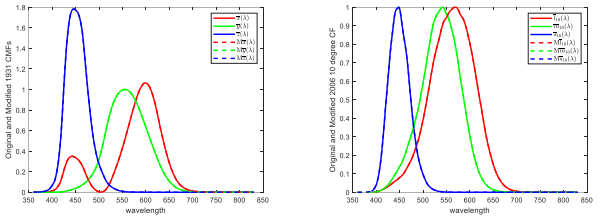

(a) (b)

Figure 6. *Original and modified CIE 1931 CMFs (a) and CIE 10-degree CFs (b) CMFs versus wavelength (horizontal axis)*

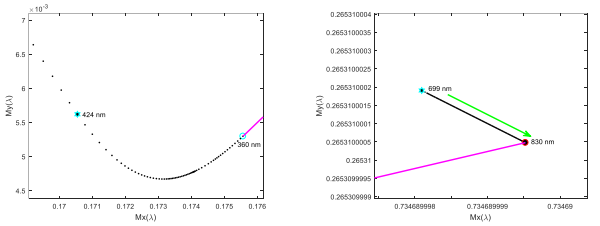

(a) (b)

Figure 7. *Enlargement of the the shorter (a) and longer (b) wavelength ranges of the chromaticity diagram derived from the $M\bar{x}(\lambda)$, $M\bar{y}(\lambda)$ and $M\bar{z}(\lambda)$*

Figure 6(b) shows the original $\bar{l}_{10}(\lambda)$, $\bar{m}_{10}(\lambda)$ and $\bar{s}_{10}(\lambda)$ with solid curves and modified $M\bar{l}_{10}(\lambda)$, $M\bar{m}_{10}(\lambda)$ and $M\bar{s}_{10}(\lambda)$ with dotted curves. Figure 8 shows the enlarged shorter (a) and longer (b) wavelength ranges of the chromaticity diagram derived from $M\bar{l}_{10}(\lambda)$, $M\bar{m}_{10}(\lambda)$ and $M\bar{s}_{10}(\lambda)$. Again, comparing with Figure 4, it can be seen that the chromaticity diagram derived from $M\bar{l}_{10}(\lambda)$, $M\bar{m}_{10}(\lambda)$ and $M\bar{s}_{10}(\lambda)$ is convex in the shorter wavelength range (see Figure 8(a)) and has no SCCs with shorter and longer wavelengths overlapping in the wavelength range from 698 nm to 830 nm (see Figure 8(b)).

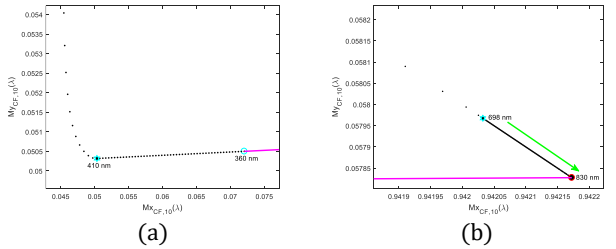

(a) (b)

Figure 8. *Enlargement of the the shorter (a) and longer (b) wavelength ranges of the chromaticity diagram derived from the $M\bar{l}_{10}(\lambda)$, $M\bar{m}_{10}(\lambda)$ and $M\bar{s}_{10}(\lambda)$*

Table 1. Wavelength ranges where the modified and original CIE CMFs and CFs are the same.

	$\bar{x}(\lambda)$ or $\bar{l}(\lambda)$	$\bar{y}(\lambda)$ or $\bar{m}(\lambda)$	$\bar{z}(\lambda)$ or $\bar{s}(\lambda)$
1931 CMFs	(424nm, 699nm)	(424nm, 699nm)	(424nm, 830 nm)
1964 CMFs	(419nm, 700nm)	(419nm, 700nm)	(419nm, 830 nm)
2° CFs	(410nm, 700nm)	(410nm, 700nm)	(410nm, 830 nm)
10° CFs	(410nm, 698nm)	(410nm, 698nm)	(410nm, 830 nm)
CMFs based on 2° CFs	(410nm, 700nm)	(410nm, 700nm)	(410nm, 830 nm)
CMFs based on 10° CFs	(410nm, 698nm)	(410nm, 698nm)	(410nm, 830 nm)

Figure 6 shows the solid and dotted curves are not overlapping for the longer wavelength range. In fact, for the shorter wavelength range the solid and dotted curves also have differences. However, these differences cannot be seen at this scale. Table 1 lists the wavelength ranges where the original and modified CMFs have no differences. Furthermore, the original CIE 2- and 10-degree CFs, and CMFs based CFs are defined between 390 nm and 830 nm. The modified versions are extended to the range from 360nm to 830nm.

Table 2. Maximum, average, and median CIELAB colour differences between original and modified CMFs and CFs evaluated using the 1269 1 nm reflectance data measured from Munsell colour chips.

	Maximum	Average	Median
1931 CMF	0.003	0.001	0.001
1964 CMF	0.004	0.001	0.001
2006 2-degree CF	0.020	0.007	0.007
2006 10-degree CF	0.018	0.007	0.007
2006 2-degree CMF	0.020	0.007	0.007
2006 10-degree CMF	0.018	0.007	0.007

Next we want to evaluate the colour differences when we use the original and modified CMFs and CFs to compute XYZ or LMS for given colour samples. To this end, we consider the 1269 1 nm reflectance data between 360 nm and 830 nm at 1 nm intervals measured from Munsell colour chips used for testing various methods for computing tristimulus values [13]. We use the CIE D65 spectral power distribution, and the CIELAB colour difference for the evaluation. Table 2 lists the maximum, average and median CIELAB colour differences. It can be seen that for 1931 and 1964 CMFs, the maximum colour differences are 0.003 and 0.004 CIELAB units respectively, while the average and median are approximately 0.001 CIELAB units. For the 2006 CFs and CMFs, we only consider the wavelength range between 390 nm and 830 nm. Furthermore, for evaluating the difference between LMS_o computed using the original CF and LMS_m computed using modified CF, we transform LMS_o and LMS_m to XYZ_o and XYZ_m using the associated transformation matrix [12], then the CIELAB colour difference between XYZ_o and XYZ_m to represent the colour difference between LMS_o and LMS_m. It can be seen that the maximum colour differences for the CIE CFs and CMFs is

approximately up to 0.02 CIELAB units and average and median CIELAB colour differences are approximately up to 0.007 CIELAB units.

Conclusions

CIE colorimetry based on colour matching functions has been successfully applied in various industrial applications. In the past it was generally accepted that the chromaticity diagram based on either 1931 or 1964 colour matching functions (CMF), contains all the chromaticity coordinates of stimuli, which means the domain (Ω) enclosed by the spectrum locus and purple line is convex. Also, based on a chromaticity diagram, the Helmholtz coordinates (dominant wavelength and excitation purity) can be defined. In this paper, the above properties of chromaticity coordinates based on CIE 1931, 1964, CIE 2006 2- and 10-degree cone fundamentals (CF) and cone fundamentals-based CMFs were evaluated. It was found that the domain Ω does not contain all the chromaticity coordinates of stimuli and spectral chromaticity coordinates do not distribute in wavelength order along the spectrum locus in the longer wavelength range, which results in errors in the determination of the Helmholtz coordinates for certain stimuli. Furthermore, modified CIE 1931, 1964 CMFs, CFs and CMFs based on CFs were derived. The modified 2- and 10-degree CFs and CMFs based on CFs were also extended down to 360 nm from original 390 nm. Finally, comparisons between the original and modified CMFs and CFs were considered. The differences between the original and modified data occur in the shorter and longer wavelength ranges (see Table 1). Using the 1269 reflectance functions measured from Munsell colour chips, and CIE D65 illuminant, for the testing it was found that the maximum colour differences (see Table 2) are 0.003, 0.004, 0.02, 0.02, 0.02, 0.02 CIELAB units between the original and modified CIE 1931, 1964 CMFs; 2°, 10° CFs; and 2°, 10° CMFs based on 2° , 10° CFs respectively.

The $V(\lambda)$ function peaks at 550 nm and decreases monotonically when λ is away from 550 nm and is nearly zero when λ is smaller than 400 nm or larger than 700 nm. Hence, visual signals were very weak when conducting visual experiments involving colour matching in the shorter and longer wavelength ranges. Thus, uncertainty at two ends of the wavelength range may cause the colour matching functions to not satisfy the two properties. The findings of this paper improve the CIE system of colorimetry and are important in the establishment of a system of colorimetry based on CIE cone fundamentals.

References

[1] CIE 15:2018, Colorimetry, Vienna, CIE (2018).

[2] ISO/CIE 11664-1:2019(E) Colorimetry — Part 1: CIE standard colorimetric observers (2019).

[3] W.D. Wright, A re-determination of the trichromatic coefficients of the spectral colours, Trans. Opt. Soc. Lond., 30, 141–164 (1928–29).

[4] J. Guild, The colorimetric properties of the spectrum, Phil. Trans. Roy. Soc. Lond., Ser. A, 230, 149–187 (1931).

[5] R.S. Berns, Billmeyer and Satzman's Principles of Color Technology, Third edition, Wiley (2000).

[6] R.W.G. Hunt and M.R. Pointer, Measuring colour, Fourth edition, Wiley (2011).

[7] R. McDonald, Colour Physics for Industry, Second edition, Society of Dyers and Colourists, Bradford, England, (1997).

[8] N. Ohta and A.R. Ronertson, Colotimetry: fundamentals and applications, Wiley (2005).

[9] CIE S 017/E:2020, INTERNATIONAL LIGHTING VOCABULARY, second edition, Vienna, CIE (2020).

[10] R.T. Rockafellar, Convex Analysis, Princeton Mathematical Series, vol. 28, Princeton University Press, Princeton, N.J., pg. 11–12 (1970).

[11] CIE Publication 170-1: 2006 Fundamental Chromaticity Diagram with Physiological Axes -Part 1: Definition of CIE 2006 Cone Fundamentals, Vienna, CIE (2006).

[12] CIE Publication 170-2: 2015 Fundamental Chromaticity Diagram with Physiological Axes- Part 2: Spectral Luminous Efficiency Functions and Chromaticity Diagrams, Vienna, CIE (2015).

[13] C.J. Li, M.R. Luo, M. Melgosa, M.R. Pointer, Testing the Accuracy of Methods for the Computation of CIE Tristimulus Values Using Weighting Tables, Color Res Appl 2016, 41(2): 125-142 (2016).

Author Biography

Cheng Gao received his BS (2015) in software engineering, MS (2018) and PhD (2023) in colour and imaging science from University of Science and Technology Liaoning China. Now he is a lecture in computer science of the same university. His research interests are colour science and imaging applications.

Kaida Xiao received his BS (1999) in computer science, MS (2000) and PhD (2007) in colour and imaging institute from University of Derby. Now he is an Associate Professor in Color and Imaging Science in the School of Design, University of Leeds, UK. He is the director of Division 1, CIE. His research interests are 3D color image reproduction and image quality enhancement.